

Insights into the Biological Redox Chemistry of 2′-Deoxyadenosine 5′-Monophosphate by Electrochemical Techniques

Rajendra N. Goyal* **and Aikta Dhawan**

Department of Chemistry, Indian Institute of Technology Roorkee, Roorkee-247 667, India

Received March 7, 2005; E-mail: rngcyfcy@iitr.ernet.in

The electrochemical oxidation of 2′-deoxyadenosine 5′-monophosphate at a pyrolytic graphite electrode (PGE) was studied in the pH range 2.65–10.03 and was found to proceed in a single well-defined oxidation peak, I_a, over the entire pH range. The cyclic voltammetric behavior indicated the pH dependence of the oxidation pathway. The kinetic studies of the UV-absorbing intermediate generated during electrooxidation were followed spectrophotometrically, and decay occurred in a pseudo first-order reaction having k values in the range $(0.595–0.986) \times 10^{-3}$ s^{-1} over the entire pH range studied. Coulometric studies indicated that the process of the oxidative pathway involved n values as 5.0 ± 0.5 in the acidic range (pH 3.37) and 4.0 ± 0.5 at physiological pH 7.22. The products of electrooxidation were characterized by GC-MS and on the basis of electrochemical, spectrochemical, and product analysis; a plausible redox mechanism is suggested.

2′-Deoxyadenosine 5′-monophosphate (2′-dAMP) is one of the deoxyribonucleotides that form a skeletal framework of the hereditary carrier DNA, and is a phosphate derivative of 2′-deoxyadenosine, a purine nucleoside.[1] It is present in the embryo of copepod Euchaeta Japonica before hatching.[2] 2′-dAMP blocks the bitter taste of foods and beverages by a pharmaceutically active oral dose that comes in contact with the taste tissues.[3] It is thus used in oral (mouth wash) formulations.[4] Fast-dissolving edible films containing 2′-dAMP are formulated to inhibit the activation of bitter taste G-protein sensory perception of bitter-tasting medicaments.[5] It is reported that 2′-dAMP on selective hydrolysis in the presence of *Xanthomonas maltophilia*, *Escherichia coli*, *Pseudomonas Putida*, and *Lactobacillus Acidophilus* leads to the formation of nucleoside 2′-deoxyadenosine with no accumulation of free bases.[6] 2′-dAMP suppresses hematologic cell growth exhibiting an anti-proliferative effect on leukemic cells.[7] It also inhibits RNAse H activity of human hepatitis B virus polymerase, and prevents the replication of human hepatitis B virus (HBV).[8] Adefovir dipivoxil (ADV) is esterologically cleaved to the 2′-dAMP analog, which upon phosphorylation acts as an anti-Hepatitis B virus (HBV) agent.[9] 2′-dAMP has been reported to prevent mitochondrial DNA depletion in a resting culture of deoxyguanosine kinase deficient fibroblast.[10] It has been reported to inhibit deoxynucleotide synthesis in chick embryos, due to which embryos usually die, or give rise to malformed chicks.[11]

2′-Deoxyadenosine 5′-monophosphate has potential as drugs for the prevention and treatment of amyloidosis, including Alzheimer's disease, by displacing the serum amyloid P (SAP) component, a glycoprotein associated with amyloid deposists.[12] In view of the importance of dAMP, adducts of a carcinogenic metabolite of 6-NC (6-nitrochrysene) with 2′-deoxyadenosine 5′-monophosphate have been synthesized in vitro.[13] Its halogenated derivative, 2-chloro-2′-deoxyadenosine 5′-monophosphate, has been separated from 2-chloro-2′-deoxyadenosine by reversed-phase HPLC.[14] The molecular conformational changes of 2′-deoxyadenosine 5′-monophosphate, induced by hexadecyltrimethylammonium bromide (NTAB) micelles and dimethyldioctadecylammonium bromide (DAB) bilayers, have been evaluated by CD spectroscopy.[15] Oxygen radicals produced in cells have been found to cause cell damage to purine nucleotides and DNA by causing hydroxylation at the C-2 position.[16] The oxidatively damaged nucleotides, particularly hydroxy derivatives, formed are incorporated into growing DNA, and have been proved to be substrate for DNA polymerases. The repair of oxidized OH radical adducts of deoxyadenosine monophosphate by phenylpropanoid glycosides has been found to be useful[17] for decreasing further oxidation of OH adducts of dAMP and dGMP. A literature survey revealed that practically no information is available concerning the oxidation of 2′-dAMP. In view of the importance of 2′-dAMP in biological systems, an attempt has been made to study the electrochemical oxidation behavior of this compound. The present work reports the results of electrooxidation studies of 2′-dAMP carried out at a pyrolytic graphite electrode (PGE).

Experimental

Material. 2′-Deoxyadenosine 5′-monophosphate (dAMP) (I) (Chart 1) was obtained from Aldrich, and was used as received. *N*,*N*-Bis(trimethylsilyl)trifluoroacetamide (BSTFA) was obtained from Sigma, and silylation-grade acetonitrile was a product of Pierce Chemical Co., U.S.A. All other chemicals used were of analytical grade. Cyclic sweep voltammetric studies were performed on a Cypress system Inc. (Ver. 7.0, Kansas, U.S.A.). The supporting electrolytes used throughout the study were phosphate buffers ($\mu = 1.0$ M) of different pH values, which were prepared according to a method of Christian and Purdy[18] from reagent-grade chemicals. The pH values of the buffer solutions were measured using a Century digital pH-meter (model CP-901-P) after due standardization.

All potentials were reported with respect to the Ag/AgCl/KCl

Published on the web October 31, 2005; DOI 10.1246/bcsj.78.1944

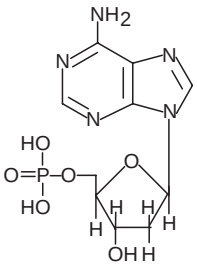

(I)

Chart 1.

(sat) electrode at an ambient temperature of 20 ± 2 °C. The working, reference, and counter electrodes were pyrolytic graphite electrode (surface area of ~6 mm^2), Ag/AgCl/KCl (sat), and platinum wire, respectively. The fabrication of the PGE used for electrochemical studies was carried out in the laboratory by a reported method.[19] After each voltammogram, renewal of the PGE surface was performed by rubbing it on emery paper, followed by washing with a jet of distilled water and gently drying with soft tissue paper. This resulted in a significantly new surface for each run, and showed a variation of ~±10% in peak currents in repeated runs. Thus, the reported peak-current values are an average of at least three runs. The number of electrons (n) involved during electrooxidation were determined by monitoring the exponential decay of the current–time curve.

UV spectral studies during the electrooxidation of 2′-dAMP and the kinetics of the UV-absorbing intermediate at the PGE were monitored by withdrawing the sample at different times. A Perkin Elmer-Lambda 35 UV–vis spectrophotometer was used for monitoring the spectra in a 1 cm cell. TLC was performed using glass plates coated with silica gel-G using benzene–methanol (4:1) as the solvent. Lyophilizer (Harrison) was used for freeze-drying of an exhaustively electrolyzed solution. GC-mass data (EI, 70 eV) were obtained on a Perkin Elmer Clares 500 Spectrometer, and HPLC analysis was carried out using an Agilent 1100 Series HPLC system.

For analysis by GC-MS, the dried extracted material (50–100 μg) was silylated with BSTFA (50 μL) and acetonitrile (50 μL) in a sealed voil and heated at 110 °C for about 12–15 min in an oil bath.[20] After cooling at room temperature, 2 μL of the silylated sample was injected in GC-MS.

Procedure. For recording voltammograms, a stock solution (1 mM) of 2′-dAMP was prepared in doubly distilled water. The stock solution (2.0 mL) was then mixed with 2.0 mL of phosphate buffer ($\mu = 1$ M) of the desired pH so that the effective ionic strength of the solution became 0.5 M. Before recording the voltammograms, the solutions were deoxygenated by passing a stream of nitrogen gas for 10–12 min.

The progress of the electrolysis was monitored by recording spectral changes at different time intervals. For this purpose, electrolysis was carried out in an H-cell at a potential 100 mV more positive than the peak potential of the oxidation peak. For recording the UV–vis spectrum, about 2–3 mL of the solution from the electrolysis cell was transferred each time to a 1 cm quartz cell, and the spectrum was recorded in the range 200–400 nm. In a second set of studies, the potential was turned off by open-circuit relaxation when the absorbance at λ_{max} was reduced to 50%. The change in absorbance with time at selected wavelengths was then monitored. The values of the rate constant (k) were calculated from linear $\log(A - A_\infty)$ versus time plots.

The products of the electrooxidation of 2′-dAMP were characterized at pH 3.37 and pH 7.22 by exhaustively electrolyzing 15–20 mg of the compound in a single compartment cell at a potential 100 mV more positive than the oxidation peak potential. The progress of the electrolysis was monitored by recording the UV spectra at different time intervals. When the oxidation peak (I_a) disappeared, the electrolyzed solution was removed from the cell and lyophilized. The products of electrooxidation were then characterized by GC-mass and HPLC analysis.

Results and Discussion

Cyclic Sweep Voltammetry. Cyclic sweep voltammetry of a 0.5 mM solution of 2′-dAMP at a sweep rate of 100 $mV\,s^{-1}$ exhibited a well-defined oxidation peak (I_a) over the entire pH range of 2.65–10.03 when the sweep was initiated in the positive direction. In a reverse sweep, no cathodic peak was obtained. A typical cyclic voltammogram of 2′-dAMP for PGE at pH 3.37 and 7.22 are presented in Fig. 1, depicting oxidation of the species generated during electrooxidation.

The peak potential of the oxidation peak (I_a) was dependent on the pH, and shifted to a less-positive potential with an increase in the pH. The E_p versus pH plot for the oxidation peak I_a was linear Fig. 2 and the dependence of E_p on the pH using a linear-regression analysis can be expressed by

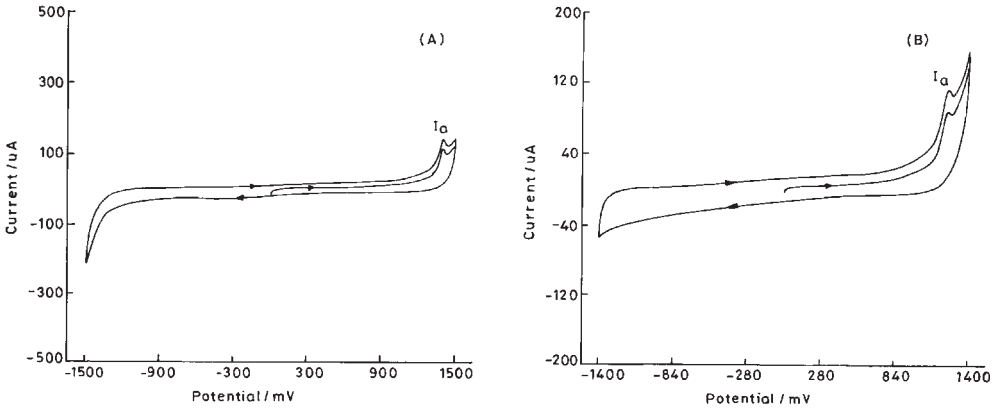

Fig. 1. Typical cyclic voltammograms observed for 0.5 mM 2′-deoxyadenosine 5′-monophosphate at sweep rate 100 $mV\,s^{-1}$ in phosphate buffers (A) at pH 3.37 and (B) at pH 7.22 at PGE.

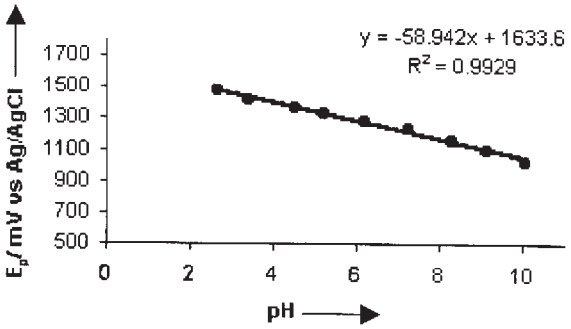

Fig. 2. Dependence of peak potential (E_p) on pH for the voltammetric peaks I_a for 0.5 mM 2′-deoxyadenosine 5′-monophosphate at sweep rate 100 mV s^{-1} at PGE.

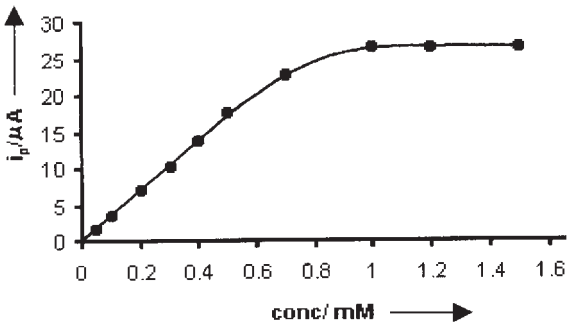

Fig. 3. Dependence of peak current (i_p) of peak I_a on concentration of 2′-deoxyadenosine 5′-monophosphate at pH 7.22, sweep rate 100 mV s^{-1} at PGE.

$$E_p(I_a) = 1633.6 - 58.942\text{pH}, \quad (1)$$

in the pH range 2.65–10.03, having a correlation coefficient of 0.993, where E_p is in mV versus Ag/AgCl. This behavior indicates the involvement of protons in the electrode process. The peak current for the peak I_a was found to increase with an increase in the 2′-dAMP concentration in the range 0.05–0.7 mM; at higher concentrations the peak current became constant Fig. 3. This behavior indicated adsorption complications in the electrode reaction.[21] The effect of the sweep rate (v) on the peak-current function of peak I_a was studied in the sweep range 20–800 mV s^{-1} at pH 7.22. A rapid increase in the $i_p/\sqrt{v}$ values with increasing sweep rate further indicate the involvement of adsorption complications, as suggested by Wopschall and Shain.[21] In the present studies, a plot of $i_p/\sqrt{v}$ versus log v was found to increase with an increase in the sweep rate, as presented in Fig. 4. The effect of the sweep rate on E_p of the peak I_a was also studied in the sweep range 20–800 mV s^{-1}. The value of E_p shifted to more positive potentials with an increase in the sweep rate, and a plot of E_p versus log v was linear with a correlation coefficient of ~0.992 (Fig. 5). This behavior is consistent with the EC nature of the reaction in which the electrode reaction is coupled with an irreversible follow-up chemical step.[22]

Coulometric Studies. The controlled potential electrolysis of 2′-dAMP was performed in phosphate buffer at pH 3.37 and pH 7.22 at a potential 100 mV more positive than peak I_a. The number of electrons (n) involved in the electrooxidation was determined by the graphical integration of the current time

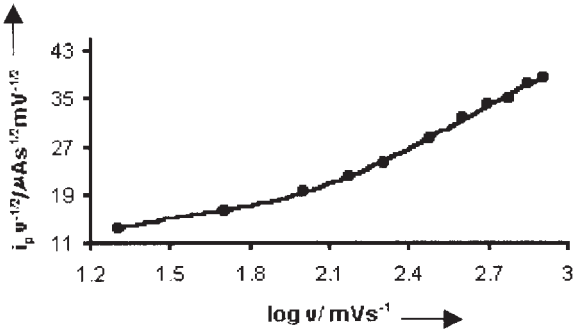

Fig. 4. Dependence of $i_p/\sqrt{v}$ on log v for peak I_a of 0.5 mM 2′-deoxyadenosine 5′-monophosphate at pH 7.22 at PGE.

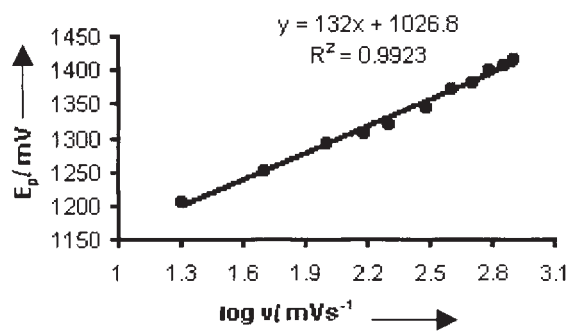

Fig. 5. Dependence of E_p on log v for peak I_a of 0.5 mM 2′-deoxyadenosine 5′-monophosphate at pH 7.22 at PGE.

curve.[23] The plot of current versus time was exponential in nature. The value of n was calculated from the net charge passed through the solution, and the average experimental value of n was found to be 5.0 ± 0.5 at pH 3.37 and 4.0 ± 0.5 at pH 7.22.

Spectral Studies. The spectral changes during the electrooxidation of 2′-dAMP were monitored at pH 3.37, 5.22, 7.22, and 9.08. The UV-spectrum of 2′-dAMP exhibited two well-defined λ_{max} at 210 and 260 nm over the entire pH range. The typical results of spectral changes observed at pH 3.37 are depicted in Fig. 6. Curve 1 in Fig. 6 is the initial spectrum of 2′-dAMP just before electrooxidation. Upon applying a potential 100 mV more positive than that of oxidation peak (I_a), the absorbance decreased systematically in the region 200–218 and 235–290 nm, as presented by (curves 2–10), whereas the absorbance in the region 218–235 nm increased systematically (curves 2–10). Two clear isosbestic points were observed at 218 and 290 nm, respectively. The decrease in absorbance at longer wavelength indicated that the formed products of oxidation of 2′-dAMP formed absorbed at smaller wavelength due to a less-conjugated nature compared with the starting material. Similar changes were observed at pH 5.22.

At pH 7.22, curve 1 in Fig. 7 shows the initial spectrum of dAMP just before electrooxidation. Upon the application of a potential of 1.4 V, the absorbance in regions 200–218 and 240–282 nm decreased, as presented by (curves 2–9), whereas in the regions 218–240 and 282–400 nm it increased systematically (curves 2–9). Three clear isosbestic points were observed at 218, 240, and 282 nm, respectively. Similar changes were also observed at pH 9.08.

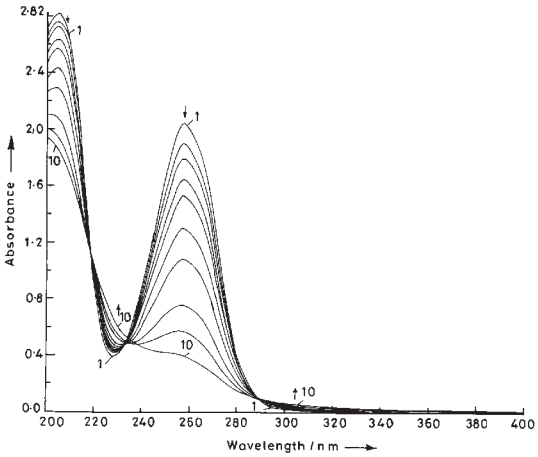

Fig. 6. Spectral changes observed during the electrooxidation of 0.5 mM 2′-deoxyadenosine 5′-monophosphate at pH 3.37 at PGE. Curves were recorded at (1) 0 min, (2) 5 min, (3) 10 min, (4) 20 min, (5) 30 min, (6) 45 min, (7) 60 min, (8) 90 min, (9) 120 min, and (10) 180 min of electrolysis.

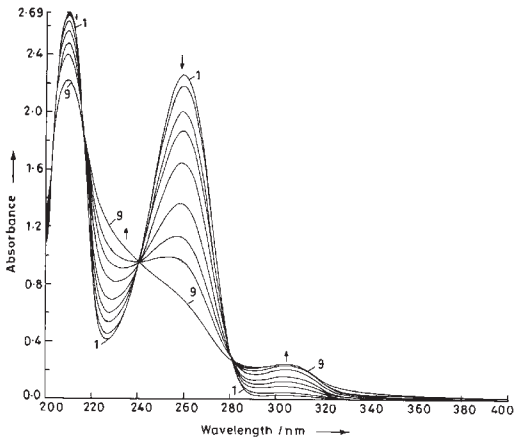

Fig. 7. Spectral changes observed during the electrooxidation of 0.5 mM 2′-deoxyadenosine 5′-monophosphate at pH 7.22 at PGE. Curves were recorded at (1) 0 min, (2) 5 min, (3) 15 min, (4) 25 min, (5) 40 min, (6) 55 min, (7) 85 min, (8) 115 min, and (9) 175 min of electrolysis.

The kinetics of decay of the UV absorbing intermediate generated was monitored after open-circuit relaxation. The changes in the absorbance with time at selected wavelengths were recorded and the resulting absorbance-versus-time profiles showed an exponential decay. The values of the pseudo first-order rate constant (k) were determined at different pH, using $\log(A - A_\infty)$ versus time plot (Fig. 8), and were found to be in the range (0.595–0.986) $\times 10^{-3}$ s^{-1}, as presented in Table 1.

Product Characterization. The ultimate products of electrooxidation of 2′-dAMP were characterized at pH 3.37 and pH 7.22. For this purpose, exhaustively electrolysed solutions of 2′-dAMP at these pH values were lyophilized. The freeze-dried material was extracted using methanol (2×10 mL) and methanolic extract was concentrated. The brownish-colored material obtained exhibited three spots in TLC in an acidic range ($R_f = 0.44$, 0.49, and 0.54), and four spots at neutral pH range ($R_f = 0.54$, 0.63, 0.68, and 0.72).

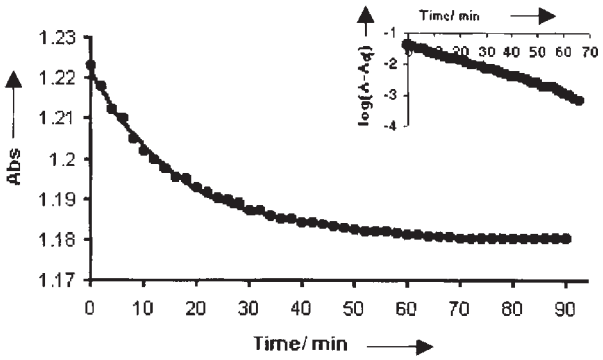

Fig. 8. Plot of absorbance versus time and $\log(A - A_\infty)$ vs time (inset) plot measured at 260 nm for the first-order decay of the UV-absorbing intermediate generated during the electrooxidation of 0.5 mM 2′-deoxyadenosine 5′-monophosphate at PGE, pH 7.22.

Table 1. Observed k Values for the Decomposition of the UV–Vis Absorbing Intermediate Generated during the Electrooxidation of 2′-Deoxyadenosine 5′-Monophosphate at PGE

pH	λ_{max}/nm	$k/10^{-3}$ s^{-1}
3.37	225	0.640
	260	0.805
5.22	225	0.626
	260	0.768
7.22	225	0.736
	260	0.986
	300	0.595
9.08	225	0.725
	260	0.946
	300	0.622

The products of electrooxidation were further characterized by HPLC and the GC-MS technique. The details of the characterized products are as follows.

In Acidic Range (pH 3.37): An HPLC analysis of the dried extracted material dissolved in methanol exhibited three peaks at $R_t \sim 2.137$, 2.284, and 2.328 min. Efforts to separate the products were not successful due to close retention times and overlapping of these peaks. The material was then silylated and analyzed by GC-MS. The GC-MS chromatogram gave four peaks at $R_t \sim 5.781$, 6.018, 9.986, and 10.563 min having m/z 449 ($M + H^+$), 465 ($M + H^+$), 908 (M^+), and 937 (M^+), respectively (Chart 2). The data giving m/z values and the relative abundance of high-mass fragments in the fragmentation pattern are summarized in Table 2.

In Neutral Range (pH 7.22): An HPLC analysis of the dried extracted material dissolved in methanol exhibited four peaks at $R_t \sim 2.124$, 2.285, 2.363, and 2.497 min. Due to a close overlapping, these peaks could not be separated. A GC-MS chromatogram of the silylated material gave four clear

1. –O-O- dimer:

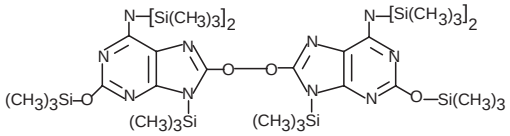

(Octasilylated)
m/z = 908
(VII)

2. –C-O-N- trimer:

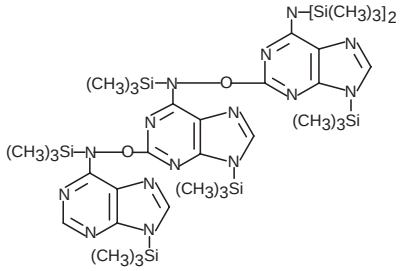

(Heptasilylated)
m/z = 937
(XXII)

3. Hydrated alloxan:

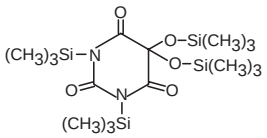

(Tetrasilylated)
m/z = 448
(XVI)

4. Urea deoxyribose:

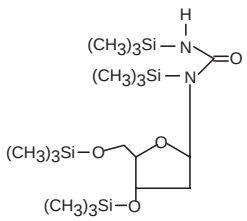

(Tetrasilylated)
m/z = 464
(XVII)

Chart 2.

1. –C-O-N- trimer:

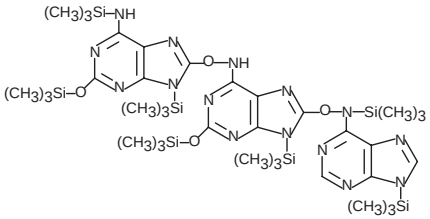

(Heptasilylated)
m/z = 969
(XXVIII)

2. –C-N-C- trimer:

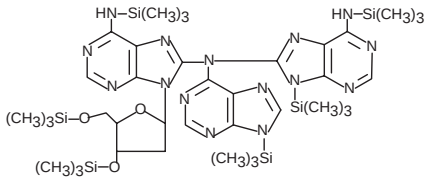

(Hexasilylated)
m/z = 949
(XXXII)

3. –C-(N-C)-C- trimer:

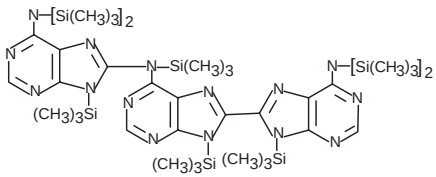

(Octasilylated)
m/z = 977
(XXXVI)

Chart 3.

peaks at $R_t \sim 6.017$, 9.986, 17.480, and 17.955 min having m/z at 970 ($M + H^+$), 908 (M^+), 950 ($M + H^+$), and 977 (M^+), respectively (Chart 3). The product corresponding to m/z 908 was found to be an –O–O– linked dimer (VII), as observed at pH 3.37. The data giving m/z values and the relative abundance of high-mass fragments are summarized in Table 3. The four major components were identified as the dimer/trimer of 2′-dAMP.

Redox Mechanism. Based on the voltammetric behavior, electronic spectral data, coulometry, and product characterization presented above, the following mechanism can be suggested for the electrooxidation of 2′-dAMP (I) at PGE.

In Acidic Media: The oxidation of 2′-dAMP (I) appears to occur in a $1e^-$, $1H^+$ step to give a free-radical moiety, II_a. The removal of $1e^-$, $1H^+$ would occur from the amino group at position 6, as was reported earlier during the oxidation of purines.[22] The free radical II_a formed has several possible resonating structures (II_a–II_e), as shown in Scheme 1. The free radicals can undergo electrodimerization by any of various mechanisms, such as radical–radical coupling or radical–substrate coupling, as shown in Schemes 1 and 2.

A parallel pathway also appears to take place for the electrooxidation of 2′-dAMP, which involves the initial $2e^-$, $2H^+$ oxidation to form either a 2-hydroxy or a 8-hydroxy derivative. However, based on studies of adenine oxidation[24] reported in the literature, it can be concluded that first $2e^-$, $2H^+$ oxidation leads to the formation of 2-hydroxy-2′-dAMP (III), which on further $2e^-$, $2H^+$ oxidation gives 2,8-dihydroxy-2′-dAMP (IV). Such an oxidation at position 8 is well-documented for purines and substituted purines.[24] The $1e^-$, $1H^+$ oxidation of 2,8-dihydroxy-2′-dAMP (IV) at position-8 to give a free-radical species (V) has been well reported[22,25] for adenosine and

Table 2. Relative Abundances Observed for High-Mass Fragments of the Peaks Observed in GC-MS at pH 3.37

R_t/min	m/z	Abundance of different fragments/%	Compound identified
9.986	908 (1.91%)	878 (1.38), 454 (1.68), 365 (3.82), 294 (5.92)	VII
5.781	449 (5.46%)	433 (2.73), 381 (2.73), 371 (4.20), 369 (2.77), 360 (0.61)	XVI
6.018	465 (3.82%)	460 (6.94), 433 (1.86), 414 (2.42), 395 (5.00), 370 (5.35)	XVII
10.563	937 (6.62%)	892 (2.46), 877 (2.55), 659 (2.42), 366 (2.55), 293 (7.50), 278 (2.81)	XXII

Table 3. Relative Abundances Observed for High-Mass Fragments of the Peaks Observed in GC-MS at pH 7.22

R_t/min	m/z	Abundance of different fragments/%	Compound identified
17.955	977 (2.53%)	917 (75.0), 904 (2.82), 627 (1.23), 467 (2.56), 190 (0.09)	XXXVI
9.986	908 (4.85%)	878 (1.46), 454 (1.76), 365 (1.24), 294 (4.78)	VII
6.017	970 (7.22%)	954 (2.56), 939 (6.08), 924 (2.56), 896 (64.0), 823 (1.47), 587 (5.28), 498 (8.85), 382 (5.45), 293 (1.41)	XXVIII
17.480	950 (8.46%)	934 (7.67), 671 (8.46), 205 (3.83)	XXXII

adenosine 5′-monophosphate. The radical species (V) immediately dimerizes with a similar moiety to form an –O–O– linked dimer (VI) through the C-8 and C′-8 positions (Scheme 1). The silylation of the dimer (VI) gave compound VII having m/z 908 corresponding to the peak at $R_t \sim 9.986$ min in a GC-MS chromatogram. It is interesting to observe that both of the deoxyribose phosphate moieties of dimer VI hydrolyze during silylation, which was also observed earlier by several workers.[22,26,27] This structure has eight reactive sites that can be replaced by $(CH_3)_3Si$ groups upon silylation. Thus, under the silylation conditions used, all of the reactive sites were occupied by the trimethylsilyl group, and an octasilylated –O–O– dimer (VII) was obtained. The oxidation of 2,8-dihydroxydeoxyadenosine (IV) can also proceed in an oxidative pathway involving a $2e^-$, $2H^+$ step to give the corresponding diimine species (IX). The diimine species (IX) obtained during the oxidation of purines was found to be unstable due to two C=N bonds, and its short half life of a few ms (~50 ms) has been already documented in the literature.[28] Hence, the diimine species (IX) will be readily attacked by water molecules to give 4,5-diol (XI). A similar attack of water molecules on diimine has been reported in the case of large a number of purines.[29,30] The formation of diol (XI) would occur in two distinct steps. An attack of the first molecule of water would occur instantaneously in a chemical follow-up step to give imine alcohol (X). Further hydration of imine alcohol (X) to give 4,5-diol (XI) would be a slow step,[31] and appears to be the step responsible for the decay observed in the first-order reaction in the absorbance vs time plot. Cleavage of the imidazole ring then occurs to give the aminopyrimidine derivative (XII), urea deoxyribose (XIII), and a phosphate moiety. A rupture of the imidazole ring of purine nucleosides in acidic medium during oxidation has been extensively reported in the literature.[32,33] The hydrolysis of compound (XII) in two subsequent steps gives hydrated alloxan (XV). The silylation of (XV) gave tetrasilylated hydrated alloxan (XVI) having m/z 448. Corresponding to the formation of XVI, a clear $M + H^+$ peak having m/z 449 and a $M^+ - 15$ peak were obtained at $R_t \sim 5.781$ min in the GC-MS chromatogram. The formation of urea deoxyribose (XIII) can be accounted for, on the basis of the peak obtained in GC-MS at $R_t \sim 6.018$ min having m/z 465, which corresponds to the $M + H^+$ peak of the silylated urea deoxyribose (XVII) with m/z 464.

The formation of compound XXI appears to be due to $1e^-$, $1H^+$ oxidation of 2-hydroxy-2′-dAMP in a side reaction to give a radical species (VIII), which rapidly combines with the II_a radical species to give XVIII. Species XVIII upon $2e^-$, $2H^+$ oxidation gives dimer XIX having a hydroxy group at the C′-2 position. The dimeric species XIX undergoes $1e^-$, $1H^+$ oxidation at the C′-2 position to give a radical species XX, which rapidly combines with the II_a radical species to form a trimer (XXI), as shown in Scheme 1. Silylation of the trimer (XXI) gave compound XXII having m/z 937, which was identified in GC-MS studies at $R_t \sim 10.563$ min. Interestingly, in compound XXII all of the three deoxyribose phosphate units were hydrolyzed during silylation, and a heptasilylated trimer (XXII) was thus obtained. Compound XXI appears to be formed as a minor product of oxidation, as judged by the relative peak area of the peak at $R_t \sim 10.563$ min.

In Neutral Media: In contrast to acidic pH, four products identified by GC-MS at pH 7.22 can be explained as follows.

In the first course of the electrooxidation of 2′-dAMP at pH 7.22, the radical species (V) formed by the overall involvement of $5e^-$, $5H^+$ as presented in Scheme 1, dimerized with a similar moiety to give VI. Thus, product VI was obtained both in acidic as well as in neutral media. Corresponding to the formation of VII in the neutral media, a clear peak having m/z 908 was noticed in the GC-MS chromatogram. The radical

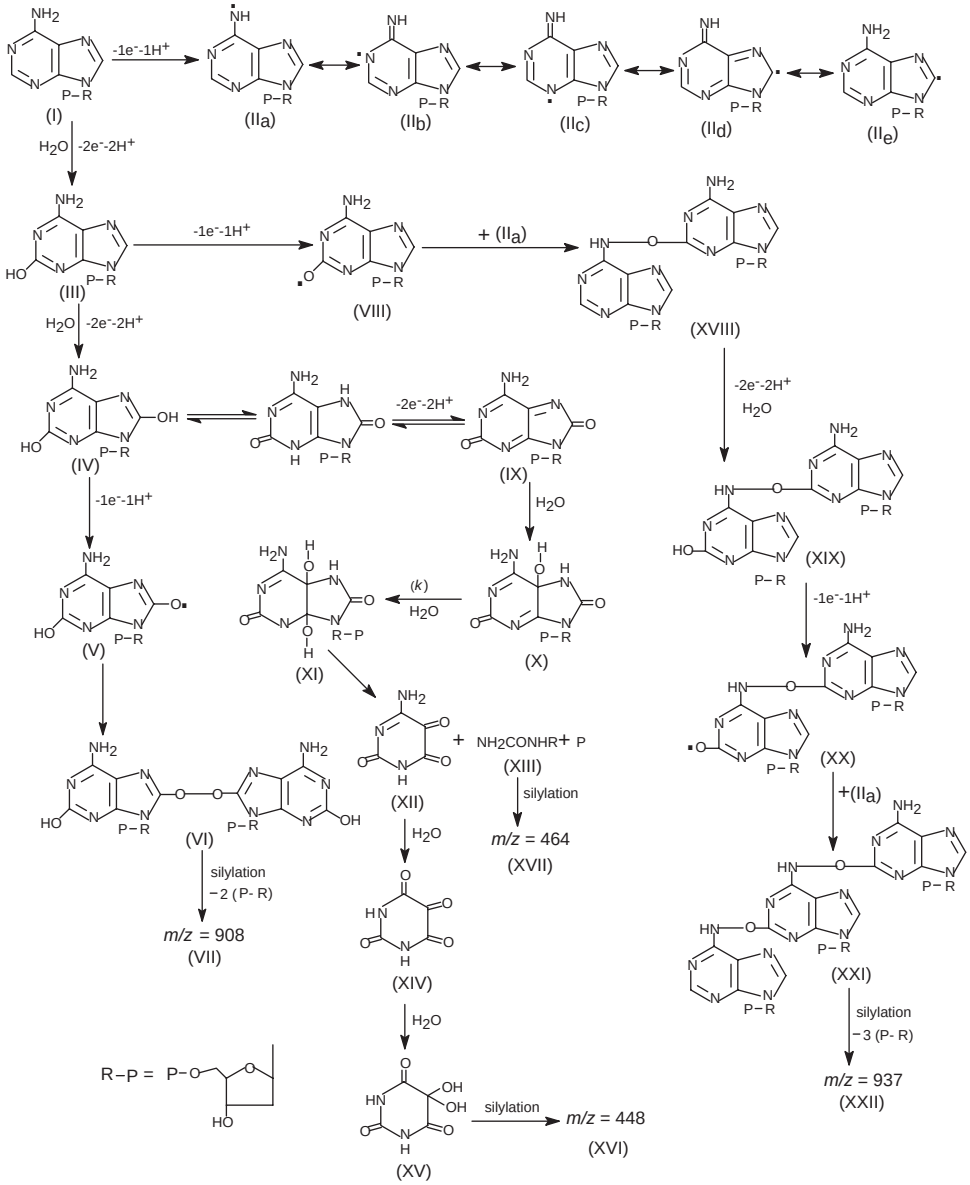

Scheme 1. Tentative mechanistic pathway proposed for the electrooxidation of 2′-deoxyadenosine 5′-monophosphate at pH 3.37.

species (V) could also combine with radical II_a to give dimer XXIII having an –O–N– linkage between the two units. The species XXIII on further $2e^-$, $2H^+$ oxidation in presence of water gave dimer XXIV having a hydroxy group at the C′-2 position. Further, $2e^-$, $2H^+$ oxidation of dimer XXIV in presence of water would give dimer XXV having a hydroxy group at the C′-8 position. Finally, XXV underwent $1e^-$, $1H^+$ oxidation at the C′-8 position to give a radical species XXVI which rapidly combined with the II_a radical species to form a trimer XXVII, as shown in Scheme 2. It is well documented in the literature that the C-8 position is more prone to oxidation compared to the C-2 position in purines.[27] The silylation of the trimer (XXVII) gave compound XXVIII having m/z 969. The peak obtained in GC-MS at $R_t \sim 6.017$ min corresponds to $M + H^+$ having m/z 970, and indicates that all three deoxyribose phosphate moieties of the trimer XXVII are removed during silylation. Although trimer XXVII has nine silylable sites, only seven underwent silylation under the conditions used. The –O–NH– hydrogen did not appear to undergo silylation under the conditions used, as observed by the observed fragmentation pattern. The high-mass peaks observed in the fragmentation pattern are compiled in Table 3.

The formation of products having m/z 949 and 977 can be explained based on the combination of radical II_e with other free radicals. The dimer XXIX, having a –C–N–C– linkage between the two units, can be formed by the combination of II_a with II_e. This dimer then undergoes $1e^-$, $1H^+$ oxidation at the –NH– position to give a radical XXX, which further combines with II_e radical to give a trimer, XXXI. Two deoxyribose phosphate moieties and a phosphate group seem to hydrolyze during silylation to give XXXII having m/z 949. The structure of XXXI has eight reactive sites, which can be replaced by $(CH_3)_3Si$ groups upon silylation. However, it was observed that under the silylation conditions used, only one hydrogen

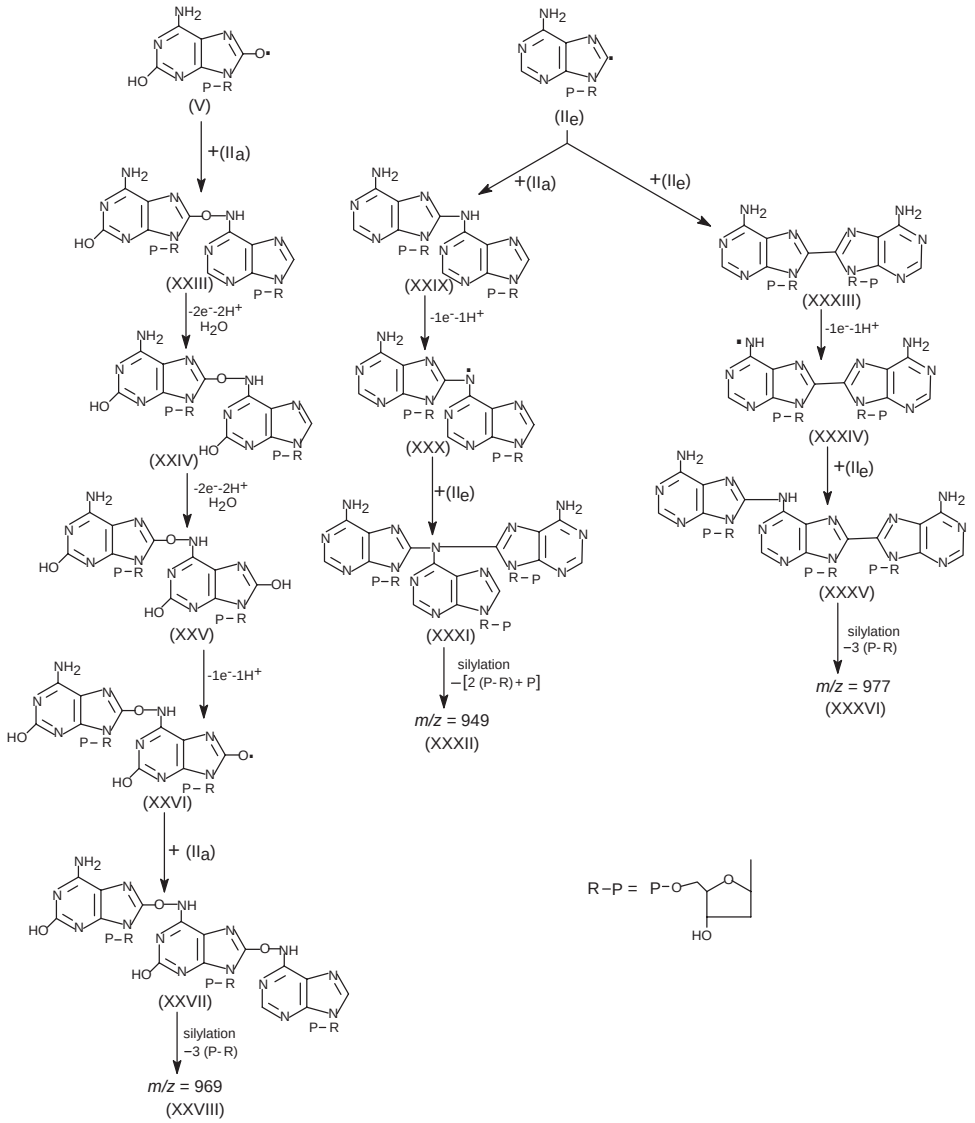

Scheme 2. Tentative mechanistic pathway proposed for the electrooxidation of 2′-deoxyadenosine 5′-monophosphate at pH 7.22.

of the amino group at the C-6 and C″-6 positions were replaced by trimethylsilyl groups to give the C–N–C trimer XXXII having m/z 949. The peak obtained in GC-MS at $R_t \sim$ 17.480 min corresponds to $M + H^+$ peak having m/z 950. The silylation of one hydrogen of the amino group in purines and their nucleosides is not uncommon, and has been reported in the literature.[26] The formation of trimer XXXV appears to be due to the combination of the radical species II_e with a similar moiety to give dimer XXXIII having a C–C linkage. This compound then undergoes $1e^-$, $1H^+$ oxidation at the amino group at position 6 or 6′, and a free radical, XXXIV, is likely to be obtained. Oxidation at –NH– at position 6 in the case of a dimer of purines is well reported in the literature.[26] The free radical XXXIV then combined with radical II_e to give a trimer, XXXV, which upon silylation gave a peak in the GC-MS chromatogram at $R_t \sim$ 17.955 min, having m/z 977. An analysis of the trimer XXXVI indicates that it is octasilylated, and all three deoxyribose phosphate units seem to hydrolyze during silylation. Moreover, the increase in the absorbance in the higher wavelength region (282–320 nm) during spectral analysis appears to be due to the formation of trimer XXXV, which possesses a highly conjugated π-system due to (C_8–C'_8) linkage, and hence absorbs at longer wavelengths.

Scheme 1 and Scheme 2 suggest the most probable routes for the formation of various products of the electrooxidation, but it should be noted that other pathways are always possible. The tentative mechanism suggested here explains all of the observed voltammetric, coulometric, and spectral data of 2′-dAMP. The formations of oxidative free radicals and dimeric purine moieties have been detected in oxidized DNAs by many workers.[34] The purine dimers produced by the coupling of free radicals generated in cellular DNA play a central role in neurodegenerative diseases, such as Alzheimer's disease, Down's Syndrome, and Xeroderma pigmentosum. To monitor the presence of such products, studies have been conducted on rabbit anti-purine dimer antiserum using purine dimer 8-8-(2′-deoxyguanosyl)-2′-deoxyguanosine 5′-monophosphate.[34] Hence, based on such studies it can be concluded that deoxyadenosine nucleosides and deoxyadenosine nucleotides are also oxidized in biosystems in a similar manner, leading to the formation of

several dimers/trimers. Thus, the present studies on the oxidative mechanism of 2′-dAMP help us to understand the nature of the intermediates and the products that can possibly form during metabolic activities in human physiology, their toxic behavior and interaction with proteins.

Conclusion

The electrooxidative mechanistic pathway of 2′-deoxyadenosine 5′-monophosphate was also compared with its parent compound, 2′-deoxyadenosine. In acidic media, 2′-dAMP upon electrooxidation led to the formation of –O–O– dimer, alloxan, urea deoxyribose, and –C–O–N– trimer, different from the products obtained on 2′-deoxyadenosine oxidation. It is interesting to observe that –O–O– dimer obtained in the case of 2′-dAMP electrooxidation lost both the moieties of deoxyribose phosphate during silylation, in contrast to the retention of both deoxyribose moieties in the case of the –O–O– dimer of 2′-deoxyadenosine. This can be accounted for due to the presence of bulky deoxyribose phosphate units, compared to simple deoxyribose. The electrooxidation of 2′-dAMP at neutral pH leads to the formation of the –O–O– dimer, –C–O–N–, –C–N–C–, and –C–(N–C)–C– trimers. The hexasilylated trimer (XXXII) formed in the present studies was similar to that obtained in the case of 2′-deoxyadenosine. This happened because of the hydrolysis of phosphate moieties during the silylation process. Thus, the suggested oxidative pathways help us to understand the mechanism of electron-transfer reactions in the biological system.

A. Dhawan is thankful to the University Grant Commission, New Delhi for the award of Junior Research Fellowship and financial assistance for the work was provided vide grant No. 6405-13-414.

References

1 G. Dryhurst, "Electrochemistry of Biological Molecules," Academic Press, New York (1977), p. 74.

2 Y. Marushige, A. S. Hepner, and M. Smith, *Can. J. Biochem.*, **8**, 5197 (1969).

3 R. A. McGregor and S. A. Gravina, U.S. Patent 86534620010525 (2001); *Chem. Abstr.*, **137**, 353261 (2002).

4 R. A. McGregor and H. D. Homan, PCT Int. Appl., US648520030303 (2003); *Chem. Abstr.*, **139**, 250023 (2003).

5 R. A. McGregor, H. D. Homan, and S. A. Gravina, PCT Int. Appl., US27111 (2003); *Chem. Abstr.*, **140**, 259084 (2004).

6 U. Chmielowiec, H. Kruszewska, and J. Cybulski, *Farmaco*, **54**, 611 (1999).

7 J. L. Vaerman, P. Moureau, F. Deldime, P. Lewalle, C. Lammineur, F. Morschhauser, and P. Martiat, *Blood*, **90**, 331 (1997).

8 L. Young, B. H. Young, K. Younhee, M. R. Hyune, and J. Guhung, *Biochem. Biophys. Res. Commun.*, **233**, 401 (1997).

9 A. S. Ray, J. E. Vela, L. Olson, and A. Fridland, *Biochem. Pharmacol.*, **68**, 1825 (2004).

10 J. W. Taanman, J. R. Muddle, and A. C. Muntau, *Hum. Mol. Genet.*, **12**, 1839 (2003).

11 H. K. Miller and M. E. Balis, *Arch. Biochem. Biophys.*, **126**, 221 (1968).

12 H. Erhard, L. H. Winston, B. P. Mark, and P. Steve, *J. Mol. Biol.*, **269**, 570 (1997).

13 J. Krzeminiski, D. Desai, J. M. Lin, V. Serebryany, K. El-Bayoumy, and S. Amin, *Chem. Res. Toxicol.*, **13**, 1143 (2000).

14 J. Bierau, R. Leen, A. H. van Gennip, H. N. Caron, and A. B. P. van Kuilenburg, *J. Chromatogr.*, **805**, 339 (2004).

15 I. L. Nantes, F. M. Correia, A. Faljoni-Alario, A. E. Kawanami, H. M. Ishiki, A. T. do Amaral, and A. M. Carmona-Ribeiro, *Arch. Biochem. Biophys.*, **416**, 25 (2003).

16 H. Kamiya and H. Kesari, *J. Biol. Chem.*, **270**, 19446 (1995).

17 Y. Li, Z. Han, S. Jiang, Y. Jiang, S. Yao, and D. Zhu, *Acta Pharmacol. Sinica*, **21**, 1125 (2000).

18 G. D. Christian and W. C. Purdy, *J. Electroanal. Chem.*, **3**, 363 (1982).

19 F. J. Miller and H. E. Zittel, *Anal. Chem.*, **35**, 1866 (1963).

20 T. R. Chen and G. Dryhurst, *J. Electroanal. Chem.*, **177**, 149 (1984).

21 R. H. Wopschall and I. Shain, *Anal. Chem.*, **39**, 1514 (1967).

22 R. N. Goyal and A. Sangal, *J. Electroanal. Chem.*, **521**, 72 (2002).

23 J. J. Lingane, "Electroanalytical Chemistry," 2nd ed, Wiley, New York (1966), p. 222.

24 R. N. Goyal, A. Kumar, and A. Mittal, *J. Chem. Soc., Perkin Trans. 2*, **1991**, 1369.

25 R. N. Goyal and A. Sangal, *J. Electroanal. Chem.*, **557**, 147 (2003).

26 P. Suramanian and G. Dryhurst, *J. Electroanal. Chem.*, **224**, 137 (1987).

27 A. A. Rostami and G. Dryhurst, *J. Electroanal. Chem.*, **223**, 143 (1987).

28 R. N. Goyal and N. K. Singhal, *Indian J. Chem. Sect. A*, **38**, 49 (1999).

29 H. A. Marsh and G. Dryhurst, *J. Electroanal. Chem.*, **95**, 81 (1979).

30 R. N. Goyal, A. B. Toth, and G. Dryhurst, *J. Electroanal. Chem.*, **239**, 1612 (1988).

31 G. Dryhurst, *J. Electrochem. Soc.*, **119**, 1659 (1972).

32 J. Wang, X. Cai, J. Y. Wang, C. Jonsson, and E. Paleck, *Anal. Chem.*, **67**, 4065 (1995).

33 R. N. Goyal, N. Jain, and D. K. Garg, *Bioelectrochem. Bioenerg.*, **43**, 105 (1997).

34 J. N. Duker, J. Sperling, J. K. Soprano, P. D. Druin, A. Davis, and R. Ashworth, *J. Cell. Biochem.*, **81**, 393 (2001).